IECO International Journal Of Industrial Electronics Control and Optimization
Print ISSN: 3517-2645
Online ISSN: 3568-2645
Homepage: https://ieco.usb.ac.ir/

Simultaneous Optimal Design of PID and MATMD Considering their Proposed Elevation Placement for Seismic Control of tall Buildings on Soft Soil

Mohammad shahi[1] | Mohammad Reza Sohrabi[1] | Sadegh Etedali[2] | Abbas-Ali Zamni[3]

Department of Civil Engineering, University of Sistan and Baluchestan, Zahedan, Iran.[1]
Department of Civil Engineering, Birjand University of Technology, P.O. Box 97175-569, Birjand, Iran.[2]
Department of Electrical Engineering, Technical and Vocational University (TVU), Tehran, Iran.[3]
Corresponding author's email: etedali@birjandut.ac.ir

Article Info

Article type:
Research Article

Article history:
Received: 21-July-2023
Received in revised form: 26-October-2023
Accepted: 28-October-2023
Published online: 30-October-2023

Keywords:
MATMD,
PID controller,
SATMD,
SSI effects,
Tall buildings,

ABSTRACT

This research proposes an innovative process to locate devices in elevation using structural results in uncontrolled and controlled (passive and active) states, considering Soil-Structure Interaction (SSI) effects, especially for soft soil. Also, a Proportional Integral Derivative (PID) controller with active single and multiple control devices is used for tall buildings under earthquakes. In addition, the simultaneous and non-simultaneous tuning of the design parameters are examined. The results of applying PID with a Multiple Active Tuned Mass Damper (MATMD) compared with the Single-Active Tuned Mass Damper (SATMD) show that the proposed process of locating the control devices reduces responses significantly. It also reduces the computational efforts of the optimization noticeably. The results of the non-simultaneous tuning of design parameters in all states also indicate an increase in the instability potential of the structure compared with simultaneous tuning. On the other hand, the reduction of the Root Mean Square (RMS) of the responses compared with the uncontrolled state confirms the effective performance of the system during earthquakes. Therefore, this research helps researchers gain a new design vision of how to locate control devices in tall buildings without optimization calculations and how to set parameters in the presence of SSI effects.

I. Introduction

Control strategies for tall buildings have received more attention in recent years. The growth of high-rise construction, efforts to reduce costs and alleviate implications for people's lives, are among the most important reasons for this attention. The tuned mass damper (TMD) is one of the conventional devices for controlling tall buildings by reducing the dynamic responses of the structure [1-5]. The single passive tuned mass damper (SPTMD) has many benefits but also some drawbacks. For instance, its performance is restricted to a specific frequency band. A common solution to overcome this problem is using a single active tuned mass damper (SATMD) [5]. Furthermore, to determine the best control force to be applied to the system without increasing the risk of instability, it is necessary to use a reliable control device and a reliable control algorithm. So far, researchers have focused on various types of controllers in their previous studies. Some classical controllers used in the control of structures, especially for tall structures, include LQG [6,7], LQR [5,8,9], H2 and H_∞ [10-12]. The controller PID [4,16,17] and its variants like fractional order PID [18-20] are a classic controller that is almost the most widely used controller in the industry. The accuracy, stability, ease of implementation, versatility, and real-time control capabilities are the PID advantages in structural control. In addition, fuzzy logic controller (FLC) [13,14,44,48] and its compounds like neuro-fuzzy logic (NFLC) [15] have been widely used in structural control topics. The advantages of fuzzy logic controllers in structural control include flexibility, ease of implementation, robustness, and interpretability, and their disadvantages of fuzzy logic controller include dependence on human expertise, difficulty in tuning, limited accuracy and computational complexity [46].

Past studies have also applied multiple passive-tuned mass dampers (MPTMD) to enhance the performance of high-rise structures against excitations by significantly reducing their dynamic responses and their potential instability [21,22]. In addition, determining the best location of MPTMD in the plan and elevation and finding the best ways to adjust its parameters have been examined [23,24]. Similar to SPTMD, the performance of MPTMD is restricted to a small range of applied frequencies. Therefore, the development of the multiple active tuned mass damper device (MATMD) has been suggested as a solution to this restriction. Structures equipped with MATMD show lower response than those equipped with SATMD, providing the best method for locating the device and the best mass value of each TMD have also been considered [21]. The reduction of the responses may result in a compromise among the displacement, acceleration, or even the relative drift ratio of the floors. An analysis of prior studies reveals that the conventional method for the best placement of multi-devices is generally the placement based on the mode shapes. [21,24,25]. Optimization methods are also used to find the optimal location in elevation [45]. At the same time, this method has a high computational cost for high-rise structures. Also, the optimal placement of TMDs in the plan has been investigated using optimization methods [47], which shows that the frequency content of the earthquake affects the optimal position of the installation of the control device. The results of using two ATMD on an 11-story structure also show that the distributed MATMD with equal mass is better than MATMD with unequal mass and single active TMD in reduction of responses [24]. TMD and controller settings are typically based on the first mode shape; It almost always guarantees a reduction in the maximum displacement of the roof but does not ensure a significant reduction in other responses. Also, the results are reasonable when most of the parameters are designed with real conditions. For example, since the soil-structure interaction (SSI) effect is one of the most important design factors, neglecting it, particularly in the case of soft soil, may increase the structure's potential for instability [4,5,26,27]. Additionally, the simultaneous or non-simultaneous-tuning of the parameters of the control device and the controller can also be one of them [14].

Also, the conditions of other items that impact the system can be considered as follows: locating the control device, changing the structure responses in elevation after applying the control, and examining the effectiveness of the control algorithm regarding the design goals.

To the best knowledge of the authors, no comprehensive research has so far been done on seismic control of high-rise buildings equipped with MPTMD or MATMD, in which the following criteria were considered together: the modes shapes, SSI effects, the placement of the devices based on the outcomes of the responses after the control of the structure by a single device, and the simultaneous and non-simultaneous tuning of design parameters.

Therefore, in this research, while examining the seismic effects of SPTMD and SATMD control devices and simultaneous and non-synchronous adjustment of design parameters, MPTMD and MATMD devices have been used considering SSI effects on a 40-story tall building. Also, an innovative process, is proposed for locating, the devices at the height of the structure. The well-known PID controller has also been used to determine the applying control signal. Then, the parameters of the devices and controller have been optimized using single and multi-objective particle swarm optimization (PSO) algorithms. Finally, the structural dynamic responses in various states and under the application of important earthquake events have been presented and evaluated.

The remainder of the paper is structured as follows. Section II presents the main structural model and the system's dynamic equations. The PID controller and its adjustment parameters are introduced in Section III. Then, Section IV describes, the PSO optimization algorithm. Section V presents the tuning results of the parameters based on artificial earthquakes. Finally Section VI discusses the analysis and evaluation of numerical results of applying real earthquakes to the structure, and Section VII provides some concluding points.

II. Structural Model

An N-story shear structure equipped with an SPTMD SATMD MPTMD or MATMD, located on the top and one other floor and subjected to an earthquake acceleration $\ddot{x}_g(t)$, is assumed.

Equipping the structure with one or two control devices considering the SSI effects added 3 or 4 degrees-of-freedom to the primary structural system. In the structural system equipped with passive or active devices, the equation of the motion of the system can be expressed as Eq. (1) and. (2), respectively[4]:

$$\boldsymbol{C}=\begin{bmatrix}[c] & [0]^T & [0]^T\\ [0] & c_s & 0\\ [0] & 0 & c_r\end{bmatrix} \quad (4)$$

$$\boldsymbol{M}\,\ddot{x}(t)+\boldsymbol{C}\,\dot{x}(t)+\boldsymbol{K}\,x(t)=-\boldsymbol{M}^*\ddot{x}_g(t) \quad (1)$$

$$\boldsymbol{M}\,\ddot{x}(t)+\boldsymbol{C}\,\dot{x}(t)+\boldsymbol{K}\,x(t)=-\boldsymbol{M}^*\ddot{x}_g(t)+\mathbf{D}u(t) \quad (2)$$

in which M, C, and K are the (N+3)× (N+3) mass, damping, and stiffness matrices of the whole system for SPTMD and SATMD and (N+4)×(N+4) for MPTMD and MATMD [4,24]; Also, $x(t)=\{x_1(t),x_2(t),\ldots,x_{N-1}(t),x_N(t),x_{d1}(t),x_0(t),\theta_0(t)\}^T$ represents the (N+3)× 1 displacement of the whole system for a single device and $x(t)=\{x_1(t),x_2(t),\ldots,x_{N-1}(t),x_N(t),x_{d1}(t),x_{d2}(t),x_0(t),\theta_0(t)\}^T$, represents the (N+4)× 1 displacement for two devices installed on the various floors, where $x_j(t)$ (j=1,..., N) are the displacement of the jth floor of the structure. $x_{d1}(t)-x_{d2}(t),x_0(t),\theta_0(t)$ refer to the TMDs stroke, displacement, and foundation rotation, respectively. In addition, $\boldsymbol{M}^*=\{m_1,m_2,\ldots,m_{N-1},m_N,m_{d1},m_0+\Sigma_{j=1}^N M_j+m_{d1},\Sigma_{j=1}^N m_j z_j+m_{d1}z_N\}^T$ or $\boldsymbol{M}^*=\{m_1,m_2,\ldots,m_{N-1},m_N,m_{d1},m_{d2},m_0+\Sigma_{j=1}^N M_j+m_{d1}+m_{d2},\Sigma_{j=1}^N m_j z_j+m_{d1}z_N+m_{d1}z_\alpha\}^T$ are the (N+3)× 1 and (N+4)× 1 acceleration mass vector for the earthquake for a system equipped with 1 and 2 control devices respectively, D is the (N+3)× 1 or (N+4)× 1 location vector of the control force, and *u(t)* is the control force applied by SATMD or MATMD to the main structure. Besides, α is the corresponding floor number on which the second device is installed. Using the Lagrangian equation, the mass matrices of the whole system are obtained as follows:

$$\boldsymbol{M}=\begin{bmatrix}[m] & \{m\} & [m]\{z\}\\ & m_0+\Sigma_{j=1}^N m_j+m_{d1}+m_{d2} & \Sigma_{j=1}^N m_j z_j+m_{d1}z_N+m_{d2}z_\alpha\\ Sym. & & I_0+\Sigma_{j=1}^N\left(I_j+m_j z_j^2\right)+m_{d1}z_N^2+m_{d2}z_\alpha^2\end{bmatrix} \quad (3)$$

where $[m]=diag(m_1,m_2,\ldots,m_{N-1},m_N,m_{d1},m_{d2})$ is the (N+2)× (N+2) mass matrix and $\{m\}=\{m_1,m_2,\ldots,m_{N-1},m_N,m_{d1},m_{d2}\}^T$ is the (N+2) ×1 mass vector of the structure equipped with MPTMD or MATMD without SSI effects. Also, $\{z\}=\{z_1,z_2,\ldots,z_{N-1},z_N,z_N,z_\alpha\}^T$ is the (N+2) ×1 elevation vector of floors. The mass, mass moment of inertia, and evaluation of the jth floor of the structure are represented by m_j, I_j, and z_j (j=1,..., N), respectively. Moreover, m_0, I_0, and m_{d1},m_{d2} are the mass and mass moment of inertia of the foundation, and mass of TMDs which are installed on different floors, respectively. To reach M, [m], and vectors $\{m\}$ and $\{z\}$ for a system equipped with SPTMD and SATMD, it is enough to vanish m_{d2} and z_α from the above matrices and vectors. The damping and stiffness matrices of the whole system are given by:

$$\boldsymbol{K}=\begin{bmatrix}[k] & [0]^T & [0]^T\\ [0] & k_s & 0\\ [0] & 0 & k_r\end{bmatrix} \quad (5)$$

where $[c]$ and $[k]$ are the (N+2)× (N+2) damping and stiffness matrices of the structure equipped with MPTMD or MATMD without SSI effects. c_s and c_r are the rocking damping and swaying damping of the foundation, and k_r and k_s refer to the rocking and swaying stiffness of the foundation. As before, to reach the matrices C and K for a system equipped with SPTMD or SATMD, the components related to device number such as k_{d2} and c_{d2} should be removed from the matrices presented above. Also, matrices $[c]$ and $[k]$ are achieved as follows:

$$[c]=\begin{bmatrix}[c_{st}]_{N\times N}+[c_d]_{N\times N} & -[c_d]_{N\times n}\\ -[c_d]_{n\times N} & [c_d]_{n\times n}\end{bmatrix} \quad (6)$$

$$[k]=\begin{bmatrix}[k_{st}]_{N\times N}+[k_d]_{N\times N} & -[k_d]_{N\times n}\\ -[k_d]_{n\times N} & [k_d]_{n\times n}\end{bmatrix} \quad (7)$$

where [c_{st}] and [k_{st}] are the main structure mass, damping, and stiffness matrices without SSI effects, respectively. Furthermore [c_d] and [k_d] are the damping and stiffness corresponding to the n-number of TMDs to be employed in the main structure. Also, the main structural system's Rayleigh proportional damping is used to calculate the damping matrix.

III. PID Controller

The PID controller has been employed in numerous engineering studies and is particularly useful for controlling tall buildings. The main benefits of this controller are its ease of use in adjusting gains and efficiency in controlling structural vibrations. [4,15,28,29]. A block diagram of the standard-form

PID controller is illustrated in Fig. 1.

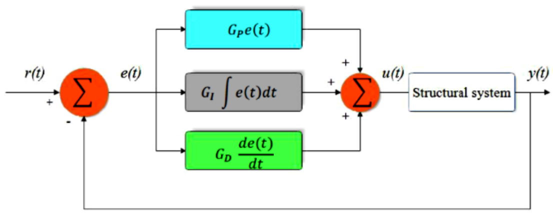

Fig. 1: The block diagram of a standard-form PID controller

According to Fig. 1, the PID controller in the time domain has an error input e(t) and is defined as e(t)= r(t)- y(t) so that r(t) is the reference input and its value is considered equal to zero in structure control issues. In addition, y(t) is the actual output value of the system. The measured error signal is the input of three separate units that create the error multiplier (proportional part), the error rate of change (differential part), and the error sum (integral part).

To determine the amount of applied control force in time t, all three components are added together and weighted by the PID control parameters (G_P, G_I, and G_D). So, the following is how the PID control force can be achieved [4,28].

$$u_{PID}(t)=G_P e(t)+G_I \int_0^t e(t)dt+G_D \frac{de(t)}{dt} \tag{8}$$

where t denotes the length of the control process and Gp, GI, and GD are the proportional, integral, and derivative terms, respectively.

IV. PSO Algorithm

PSO is a population-based stochastic optimization algorithm proposed based on the behavior of swarms in nature such as birds and fish [30]. The PSO algorithm has been used by researchers in the field of vibration control, especially in structural engineering [4,31-36,43]. The advantages of PSO over other optimization algorithms, including the genetic algorithm (GA) and the ant colony algorithm (ACO), include the small number of tuning parameters, ease of application, rapid convergence, and relatively low computational effort [4,31,34-40].

The status of a particle in the search space can be characterized by two factors: position and velocity. Considering a d-dimensional search space, the position and the velocity of the ith particle can be represented by the vectors $x_i = (x_{i1}, x_{i2}, \dots, x_{id})$ and $v_i = (v_{i1}, v_{i2}, \dots, v_{id})$, respectively. Each particle has its own best position (pbest) $p_i = (p_{i1}, p_{i2}, \dots, p_{id})$ corresponding to the personal best objective value obtained so far at time t. The global best particle is also represented as g, which denotes the best position found so far at time t in the whole swarm. The new velocity of each particle and the position of the ith particle are then updated using Eq. (9) and (10), respectively [42].

$$v_{ij}(t+1) = wv_{ij}(t) + c_1 r_1 [p_{ij} - x_{ij}(t)] \dots \tag{9}$$
$$+c_2 r_2 [g_j - x_{ij}(t)], \quad j = 1, 2, \dots, d$$

$$x_{ij}(t+1) = x_{ij}(t) + v_{ij}(t+1), \quad j = 1, 2, \dots, d \tag{10}$$

where the acceleration coefficients, denoted by the constants $\boldsymbol{c_1}$ and $\boldsymbol{c_2}$, are frequently set to 2.0 based on prior knowledge. Moreover, w is the inertia weight factor, which is frequently in the range [0.1, 0.9] and can be obtained using the updated following equation to improve convergence: $\boldsymbol{r_1}$ and $\boldsymbol{r_2}$ are two independent random numbers uniformly distributed in the range [0, 1].

$$w = w_{max} - n_i \left(\frac{w_{max} - w_{min}}{n_{max}}\right) \tag{11}$$

in which $\boldsymbol{w_{max}}$ and $\boldsymbol{w_{min}}$ denote maximum and minimum weights. Also, $\boldsymbol{n_i}$ and $\boldsymbol{n_{max}}$ are the current generation number, and the maximum number of generations, respectively [41].

V. Numerical Studies

A well-known 40-story benchmark structure has been chosen to investigate how well a tall building performs against earthquakes when equipped with one or more control devices, such as SPTMD, SATMD, MPTMD, or MATMD [1,4].

Because studying SSI effects is more crucial in soft soils than other soils, this state was selected as a construction soil for all designs. The specifications of the main structure are shown in Table 1. Table 2 presents the soft soil parameters.

A. *Proposed placement of TMDs*

Previous studies have optimally located the control device using mode shapes. In the present research, with an innovative process and according to [4], other items were included in the design process as follows: the results of uncontrolled state and controlled state by SPTMD and SATMD considering SSI effects.

The first eight modes are shown in Fig. 2. Also, the normalized maximum deformation of the modes and the corresponding floors are presented in Table 3. Based on [4], Fig. 3 displays the diagram of the relative displacement, acceleration, and drift ratio of the structure floors under a filtered white noise artificial earthquake for various states in which w/o control, PTMD, and PID1US show, the uncontrolled state, controlled state by a single passive TMD and single ATMD in non-simultaneous tuning, respectively. As was already mentioned, the single device is installed on the top floor. It is evident from Fig. 2 and Table 3, that the top story is where the structure's maximum displacement occurs. It confirms the 40th floor's selection as the best location to limit the maximum displacement of the structure. This conclusion is confirmed in Fig. 3, containing before and after controlling. Furthermore, for the uncontrolled and SPTMD states, the maximum acceleration has occurred on the 24th floor. On the other hand, it is the 25th floor for the SATMD state. Additionally, the highest value of the relative drift ratio of the floors is related to the 33rd floor for the uncontrolled and SATMD, the 32nd floor for the SPTMD.

TABLE 1
STRUCTURAL PARAMETERS [1,4]

Number of stories	40
Story height	4 m
Breadth and depth of the structure	40 m
Story mass, mass moment of inertia	m_j=9.80e5 kg, I_j=1.31e8 kg.m2
Story stiffness*	k_1= 2.13 e9 N/m, k_{40}=9,98e8 N/m
Foundation radius, mass, moment of inertia	R_0=20m, m_0=1.96e6kg, I_0=1.96e8kg.m2

* The stiffness of each story is linearly decreased as the evaluation of the structure

TABLE 2
THE SOFT SOIL PARAMETERS [1,4]

Soil type	Poisson's ratio (ν_s)	Soil density $\rho(kg/m^3)$	Shear wave velocity $V_s(m/s)$	Shear modulus $G_s(N/m^2)$	Swaying damping $(N.s/m)$	Rocking damping $C_r(N.s.m)$	Swaying stiffness $K_s(N/m)$	Rocking stiffness $K_r(N.m)$
Soft	0.49	1800	100	1.80×107	2.19×108	2.26×1010	1.91×109	7.53×1011

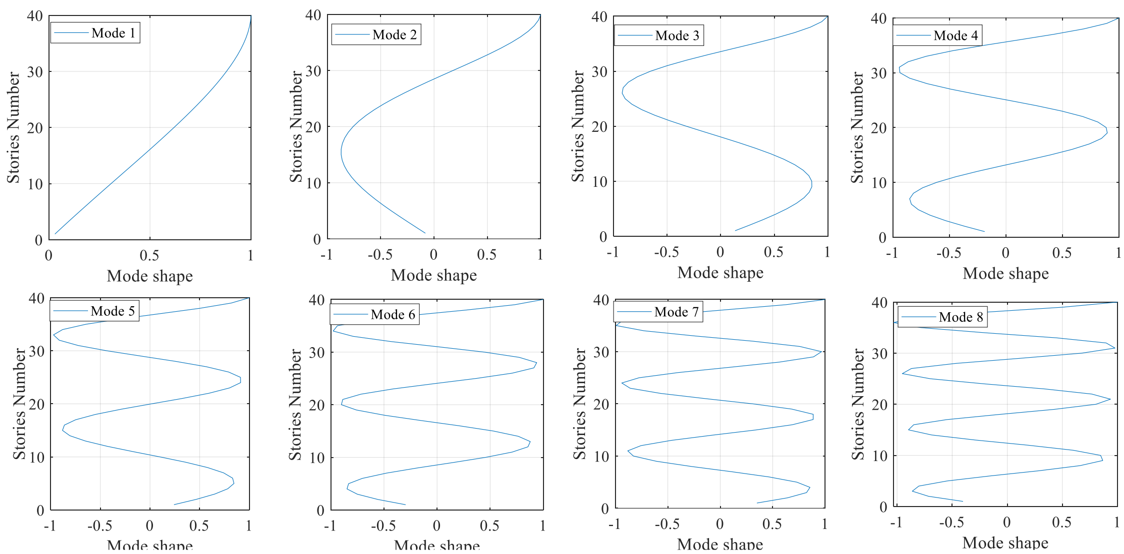

Fig. 2. The 1st to the 8th normalized mode shapes

TABLE 3
THE RESULTS OF THE MODE SHAPES ANALYSIS

Mode number	**1**	**2**	**3**	**4**	**5**	**6**	**7**	**8**
Maximum Deformation(normalized)*	1	1	1	1	1	1	1	1.03
Corresponding floor	40	40	40	40	40	40	40	36

*Max. floor deformation normalized by 40th-story deformation

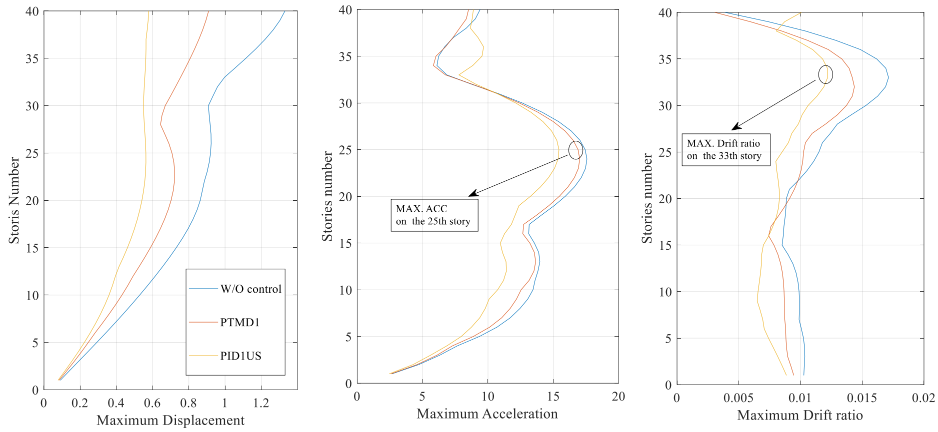

Fig. 3. The maximum responses of a structure subjected to an artificial earthquake [5]

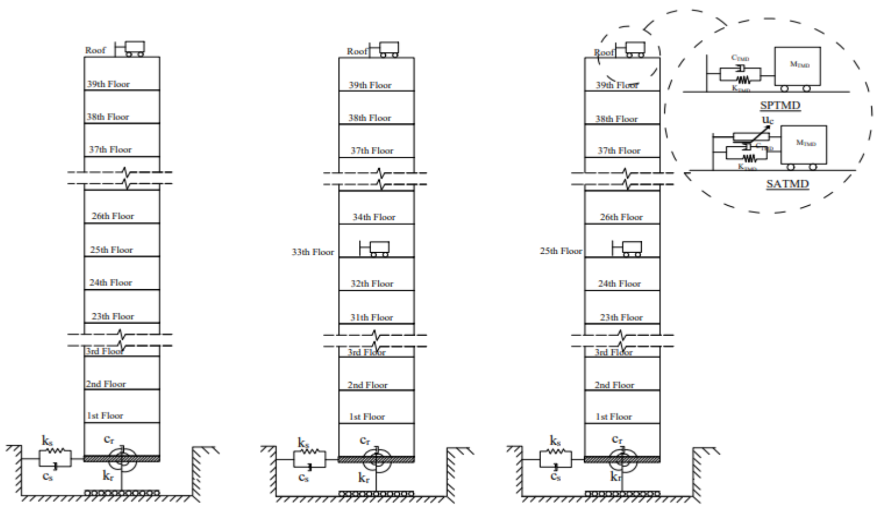

(a) (b) (c)

Fig. 4. The proposed location for installing various control devices on the elevation of the structure: (a) single device, (b) multi-device-case40-33, (c) multi-device-case40-25

According to all the aforementioned factors, it can be proposed that the 40th floor is the fixed best location for one of the control devices. To locate the second device, we should accept the possible compromise between reducing displacement-acceleration and displacement-relative drift which leads to two possible scenarios, henceforth named case 40-33 and case 40-25. The numbers after the case refer to the location of devices on floors. Fig. 4 shows the suggested location for the structure equipped with a single control device (SPTMD or SATMD) and multiple devices (MPTMD or MATMD).

B. *Optimal TMD and PID parameters*

Different states of controller and control device parameter optimization using the PSO algorithm have been examined. The evaluation of the effects of using one or more control devices(passive or active) and the effect of simultaneous and non-simultaneous tuning of TMDs and PID parameters are among them. In this study, the meaning of non-simultaneous tuning is that first, using the optimization algorithm, the optimal tuning of the parameters TMD and then the optimal tuning of the PID controller parameters is done. On the other hand, simultaneous tuning means tuning the devices and controller parameters at the same time under an artificial earthquake. The first optimization problem involves finding the best TMD parameters for two states of TMD placement. The first state includes SPTMD and SATMD, and the second includes MPTMD and MATMD. The optimal design of TMD parameters for multi-control devices, including frequency ratios, f_1, f_2, and damping ratios, ξ_{T1}, ξ_{T2}, with various mass ratios of TMD is as follows:

$$\begin{cases} Find \quad x = \{f_1, \xi_{T1}, f_2, \xi_{T2}\} \\ \text{minimize} \quad \mathrm{F} = (Of_1, Of_2) \end{cases} \tag{12}$$

Also, assuming that M_s is the mass of the original structure, the optimum TMDs mass, damping, and stiffness of TMDs are calculated as follows:

$$\begin{cases} M_{tmd1} = \gamma_1 M_s \\ \quad and \\ M_{tmd2} = \gamma_2 M_s \end{cases}, \begin{cases} C_{tmd1} = 2M_{tmd1}\xi_{T1} f_1 \omega_s \\ \quad and \\ C_{tmd2} = 2M_{tmd2}\xi_{T2} f_2 \omega_s \end{cases}, and \begin{cases} K_{tmd1} = M_{tmd1} f_1^2 \omega_s^2 \\ \quad and \\ K_{tmd2} = M_{tmd2} f_2^2 \omega_s^2 \end{cases} \tag{13}$$

where, γ_1 and γ_2 are preselected mass ratios of TMDs. The second optimization problem entails designing a PID controller to adjust the control force for SATMD and MATMD as follows, respectively:

$$\begin{cases} Find \quad \mathrm{x} = \{G_{P1}, G_{I1}, G_{D1}\} \\ \text{minimize} \quad \mathrm{F} = (\,Of_1\,) \\ Subjected\ to\ \ \max\|u_{PID1}(t)\| \le 0.05\ \mathrm{W_s} \end{cases} \tag{14}$$

$$\begin{cases} Find \quad \mathrm{x} = \{G_{P1}, G_{I1}, G_{D1}, G_{P2}, G_{I2}, G_{D2}\} \\ \text{minimize} \quad \mathrm{F} = (\,Of_1, Of_2\,) \\ Subjected\ to\ \ \max\|u_{PIDi}(t)\| \le 0.05\ \mathrm{W_s} \quad \mathrm{i} = 1, 2 \end{cases} \tag{15}$$

in which, G_{P1}, G_{I1}, G_{D1}, G_{P2}, G_{I2}, G_{D2} are the parameters related to two controllers corresponding to control devices installed in different floors. The total weight of the structure is represented by W_S. Also, the search spaces of f_i, ξ_{Ti} , G_{Pi}, G_{Ii}, G_{Di} parameters for the upper and lower bands are limited, based on previous experience, to [0.5, 1.4], [0.01,0.2], [9e4,12e4], [1.7e8,2.2e8], [0,2e3], respectively.

In Eq. 12-14, only subscript 1 is considered for the state of SPTMD or SATMD and the rest of them are ignored. For SPTMD Eq. 12-13, and for SATMD, Eq. 12-14 are considered a single-objective optimization. In Eq. 12 and 14, only of_1 is considered the single-objective function.

In other words, for MPTMD Eq. 12-13 and for MATMD, Eq. 12-13 and 15 are considered a multi-objective optimization. The population size for single-objective and multi-objective optimization is 50 and 100, respectively; In addition, the prescribed number of iterations is considered equal to 20 for both states.

As mentioned in Section 5.1, cases 40-25 and 40-33 have been proposed to investigate the effects of control device placement. In Eq. 12 and 15, the two-objective function includes minimizing the maximum displacement of the roof floor (Of_1) and the maximum acceleration of the 25th floor (Of_2) corresponding to case 40-25. Similarly, for case 40-33, the multi-objective function includes minimizing the roof displacement(Of_1) and relative drift ratio (Of_2) of 33rd floor. For the mass ratio of TMDs, three scenarios are proposed. The main constraint for determining the mass of TMDs is $\sum_{i=1}^{i=2} M_{TMD_i} = 0.05 \times M_S$. It has been proposed to compare with the single device state. The recommended mass ratios for the TMD installed on the 40th floor are three values of γ_1=4, 3, and 2.5%. For the device installed on the 25th or 33rd floor, the corresponding values of γ_2=1, 2, and 2.5% are suggested. In other words, the combination of mass ratios of 4%-1%, 3%-2%, and 2.5%-2.5% has been selected for the γ_1 and γ_2 values, respectively.

For generalizing settings and avoiding several time-consuming analyses, an artificial earthquake has been applied for tuning control parameters. The filtered white noise is used as the artificial earthquake. It is generated by passing a Gaussian white noise process through a filter model [4]. The well-known Kanai-Tajimi filter with the following spectral density function is applied for this purpose [4,16].

$$s(\omega) = S_0 \left[\frac{{\omega_g}^4 + 4{\xi_g}^2{\omega_g}^2\omega^2}{(\omega^2 - {\omega_g}^2)^2 + 4{\xi_g}^2{\omega_g}^2\omega^2} \right], \quad S_0 = \frac{0.03\xi_g}{\pi\omega_g(4{\xi_g}^2 + 1)} \tag{15}$$

where S_0, ξ_g, and ω_g are the constant spectral density, the ground damping, and frequency, respectively. In this paper, $\xi_g = 0.3$ and $\omega_g = 37.3\ rad/s$ have been used for numerical simulations. The filtered white noise is shown in Fig. 5. The Optimum TMD and PID parameters for SPTMD and SATMD and the non-simultaneous tuning state are inserted in Table 4 [4]. Also, the results of the simultaneous tuning of them are inserted in this table. The best results of optimal design for MATMD, MPTMD, and PID parameters are presented in Tables 5 and 6; They have been extracted based on the Pareto diagram, considering a compromise between the responses. In addition, the optimal parameters with various proposed placements and different mass ratios have been inserted. In Table 5, the optimal PID parameters are obtained in the continuation of fixing the optimal TMD parameters. In contrast, all parameters presented in Table 6 have been optimized simultaneously.

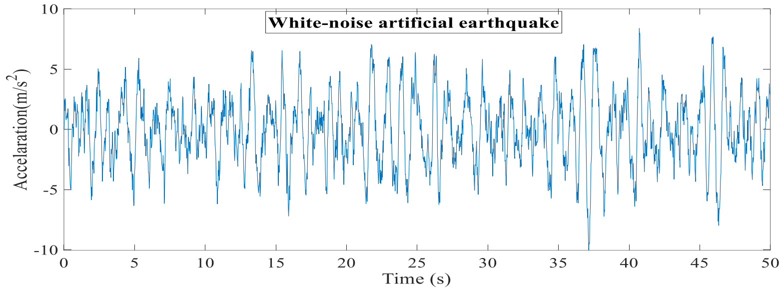

Fig. 5. The filtered white noise artificial earthquake

TABLE 4
OPTIMUM TMD AND PID PARAMETERS FOR SOFT SOIL [4]

Tuning type	TMD parameters		PID parameters		
	frequency ratio (f)	damping ratio (ξ_T)	G_P	G_I	G_D
Non-simultaneous [4]	1.26	0.20	1.10×10^5	1.94×10^8	0.00
Simultaneous	1.22	0.08	1.11×10^5	1.79×10^8	1.06×10^3

TABLE 5
OPTIMUM TMD AND PID PARAMETERS FOR SOFT SOIL (NON-SIMULTANEOUS TUNING)

Case	**TMD location (story)**	**TMD mass ratio**	**TMD parameters**		**PID parameters**		
			frequency ratio (f)	**damping ratio (ξ_T)**	G_P	G_I	G_D
40-33	40	4%	1.3967	0.1996	1.0 e+05	1.7 e+08	0.0
	33	1%	0.7303	0.1956	1.0 e+05	1.7 e+08	0.0
	40	3%	1.3806	0.1965	1.0 e+05	1.7 e+08	1.6788e+03
	33	2%	0.9555	0.1972	1.0 e+05	1.7 e+08	978.5679
	40	2.5%	1.3796	0.1902	1.0 e+05	1.7 e+08	705.4445
	33	2.5%	1.0049	0.0940	1.0 e+05	1.7 e+08	511.3972
40-25	40	4%	1.400	0.1905	1.0243e+05	1.7341e+08	1.7150e+03
	25	1%	0.6137	0.0100	1.0492e+05	1.7043e+08	1.6726e+03
	40	3%	1.3902	0.1992	1.1410e+05	1.7275e+08	518.8052
	25	2%	0.6230	0.1969	1.0131e+05	1.7552e+08	1.7085e+03
	40	2.5%	1.400	0.2000	1.0 e+05	1.7 e+08	240.7838
	25	2.5%	0.6000	0.1854	1.0 e+05	1.7 e+08	673.5438

TABLE 6
OPTIMUM TMD AND PID PARAMETERS FOR SOFT SOIL (SIMULTANEOUS TUNING)

Case	**TMD location (story)**	**TMD mass ratio**			**PID parameters**		
			frequency ratio (f)	**damping ratio (ξ_T)**	G_P	G_I	G_D
40-33	40	4%	1.2298	0.0887	727.6826	1.8569e+08	1.1308e+05
	33	1%	0.7466	0.0274	1.2826e+03	1.8142e+08	1.1072e+05
	40	3%	1.1903	0.0912	1.0 e+05	1.8990e+08	0.0
	33	2%	0.7810	0.1121	1.0 e+05	2.0825e+08	1.1679e+03
	40	2.5%	1.4000	0.2000	1.9240e+03	2.1962e+08	1.0364e+05
	33	2.5%	0.6262	0.1891	2.0 e+03	1.7217e+08	1.2 e+05
40-25	40	4%	1.4000	0.1849	1.0457e+03	1.9321e+08	1.1998e+05
	25	1%	0.6031	0.0494	781.6318	1.9691e+08	1.0 e+05
	40	3%	0.6621	0.1880	470.4099	1.7097e+08	1.1064e+05
	25	2%	1.4000	0.2000	1.7688e+03	1.7 e+08	1.1762e+05
	40	2.5%	0.6382	0.2000	276.8684	1.7409e+08	1.0 e+05
	25	2.5%	1.4000	0.2000	1.9685e+03	1.9258e+08	1.0278e+05

VI. Results and Discussion

The findings of [4] are utilized to assess the effectiveness of the proposed change. The evaluation of the suggestions, such as locating control devices in the elevation, how to choose the best design parameters, simultaneous and non-simultaneous settings of devices and controller parameters, and the TMDs mass various ratios, was explored. Table 8 presents the comparative results under artificial earthquake for all proposed cases. Fig. 6 illustrates the results of a filtered white noise earthquake application for case 40-33 and different mass ratios. All figures depict uncontrolled (w/o control), the structure equipped with an SPTMD (PTMD1), an SATMD and PID controller with non-simultaneous settings (PID1US), an SATMD and PID controller with simultaneous settings (PID1S), MPTMD with two TMDs (PTMD2), MATMD with two devices PID controller with non-simultaneous settings (PID2US), and finally MATMD with two devices and PID controller with simultaneous settings (PID2S), respectively. In Fig. 6, subcase 4-1 is related to the mass ratio of the TMD device, which is located on the 40^{th} and 33^{rd} floors, respectively. Similarly, subcases 3-2 and 2.5-2.5 are also defined. Table 8 shows the maximum displacement response when using the SATMD. Simultaneous tuning is improved by 7.1% compared with the non-simultaneous state. At the same time, there is little change in the maximum acceleration and maximum drift ratio of the floors. Furthermore, there are no appreciable differences in responses when MPTMD is used instead of SPTMD.

As well, the results of the non-simultaneous tuning of MATMD and PID controller show a decrease of up to 14.3% compared with the uncontrolled state, whereas, compared with the SATMD with non-simultaneous tuning, an increase of up to 183.7% can be seen in responses. Of course, in the case of the maximum acceleration of the floors, the results of the answers are almost unchanged. On the other hand, the results of the simultaneous settings show a reduction of the maximum displacement up to 67.7% compared with the uncontrolled case. This decrease is 19.9% compared with SATMD with non-simultaneous tuning, which is related to case 40-33 with a mass ratio of 4%-1%. Also, the improvement of the response of the maximum acceleration and the maximum drift ratio is 25.4% and 40.4% compared with the uncontrolled case. This decrement is 15.3% and 16.4% compared with SATMD with non-simultaneous adjustment, which belongs to case 40-25 with a mass ratio of 4%-1%. The results show that the decrement of the maximum acceleration occurs in all states. At the same time, by considering a trade-off between the reduction of the maximum responses, the best result may belong to case 40-25 or case 40-33 and the mass ratio of 4%-1%. The corresponding percent is up to 19.9%, 15.3%, and 16.4% compared with SATMD, respectively.

Compared to [4], the general evaluation of the results demonstrates significant improvement in responses all over the cases, including structures equipped with SATMD and MATMD with simultaneous tuning. In addition, it shows that the proposed placements of devices were successful compared with the control primary objectives.

The optimal settings were evaluated by two famous Kobe and Northridge (Newhall station) earthquakes. they were reported by [4], and their characteristics are given in Table 7. From now on, the earthquake is referred to as Northridge (Newhall station) abbreviated as Newhall. Also, the data of these earthquakes have been extracted from the PEER Ground Motion Database. Tables 9 and 10 report the results of these earthquakes. Additionally, Fig. 7 displays the results of dynamic responses to the Kobe earthquake. For the simultaneous settings of SATMD and PID compared with non-simultaneous settings [4], the results of applying the Kobe-1995 and Northridge-1994 earthquakes show a reduction of 6.4% and 14.4% in the maximum displacement, respectively. Furthermore, the maximum acceleration for Kobe was almost unchanged and for Newhall, an increase of 8.5% was seen. An increase of 17.5% for Kobe and 16.1% for Newhall occurred in the maximum floor drift.

The examination of the results of the application of MPTMD on the structure for all cases shows insignificant changes compared with the SPTMD state. This general conclusion is true for two earthquakes and all maximum responses. Also, the analysis of the results of the responses of the structure equipped with MATMD with the non-simultaneous tuning reveals decreases of up to 19% and up to 39.4% for the results of the Kobe and Newhall earthquake compared with the uncontrolled state in the maximum displacement, respectively. The maximum acceleration and maximum drift for all cases are almost lower than those in the uncontrolled state, except for Kobe and maximum acceleration for case 40-25.

TABLE 7
THE CHARACTERISTICS OF EARTHQUAKES

Earthquake Name	Year	Magnitude	Station Name	PGA(g)
Kobe	1995	6.9	KJMA	0.82
Northridge	1994	6.69	Newhall	0.59

Almost all responses mentioned above are incremental compared with the SATMD with non-simultaneous settings. Only in Kobe and case 40-25, did the responses improve significantly.

The best results for Kobe are related to the maximum displacement of MATMD with simultaneous setting, which belongs to case 40-33 with a mass ratio of 3%-2%. Also, a reduction of 53.7% and 26.5% were reported compared with the uncontrolled state and SATMD with non-simultaneous tuning, respectively. In this regard, the maximum decrement for the maximum acceleration and the maximum drift ratio of floors belongs to case 40-33 which are, 11.3% and 16.7% compared with the uncontrolled state and 5.9%, and 4.8% compared with the SATMD and non-simultaneous setting, respective. In contrast, the same increment is reported for case 40-25 so that the maximum acceleration increase by up to 8.4%.

TABLE 8
RESULTS FOR ALL CONTROL CASES UNDER THE ARTIFICIAL EARTHQUAKE

Control case	Subcase	Non-simultaneous tuning			Simultaneous tuning		
		MAX. Disp(m)	MAX. Acc(m/s^2)	MAX. Drift ratio	MAX. Disp(m)	MAX. Acc(m/s^2)	MAX. Drift ratio
Uncontrolled	-	1.33	17.57	0.017	-	-	-
SPTMD [4]	-	0.91(31.7%)	17.02(3.1%)	0.014(15.8%)	-	-	-
SATMD (Un-simultaneous) [4]	-	0.58(56.7%)	15.43(12.18%)	0.012(28.6%)	-	-	-
SATMD (Simultaneous)	-	-	-	-	0.54 (59.7%,7.1%)*	15.46 (12.0%, -0.2%)	0.012 (28.7%, 0.0%)
MPTMD (case 40-33)	4-1	0.91 (31.5%)	17.03(3.1%)	0.014 (17.0%)	-	-	-
	3-2	0.92 (30.8%)	17.25(1.8%)	0.014 (15.8%)	-	-	-
	2.5-2.5	0.93 (30.4%)	17.38(1.8%)	0.015 (14.0%)	-	-	-
MPTMD (case 40-25)	4-1	0.91 (31.3%)	16.80(4.4%)	0.015 (11.7%)	-	-	-
	3-2	0.93 (30.4%)	17.10(2.6%)	0.015 (12.3%)	-	-	-
	2.5-2.5	0.93 (30.0%)	17.16(2.3%)	0.015 (10.5%)	-	-	-
MATMD (case 40-33)	4-1	1.52 (-14.2%, -183.7%)	16.04 (8.7%, -3.7%)	0.016 (3.5%, -35.2%)	**0.43 (67.7%, 19.9%)**	13.88 (21.0%, 10.2%)	0.012 (26.9%, -2.5%)
	3-2	1.48 (-10.9%, -175.5%)	15.92 (9.4%, -2.9%)	0.016 (4.1%, -34.4%)	0.46 (65.5%, 14.2%)	13.92 (20.8%, 10.0%)	0.012 (28.7%, 0.0%)
	2.5-2.5	1.518 (-13.6%, -182.1%)	15.92 (9.4%, -3.0%)	0.016 (4.15, -34.4%)	0.44 (67.2%, 18.6%)	13.67 (22.1%, 11.6%)	0.012 (28.7%, 0.0%)
MATMD (case 40-25)	4-1	1.148 (14.3%, -113.0%)	15.37 (12.5%, 0.6%)	0.015 (9.9%, -26.2%)	0.53 (60.4%, 1.7%)	**13.10 (25.4%, 15.3%)**	**0.010 (40.4%, 16.4%)**
	3-2	1.148 (14.2%, -113.1%)	15.51 (11.7%, -0.3%)	0.016 (9.4%, -27.0%)	0.55 (59.0%, -1.9%)	14.02 (20.2%, 9.4%)	0.012 (27.5%, -1.6%)
	2.5-2.5	1.26 (5.6%, -134.4%)	15.59 (11.35, -0.8%)	0.017 (1.2%, -38.5%)	0.55 (58.8%, -2.4%)	14.24 (18.9%, 7.9%)	0.013 (26.3%, -3.3%)

Note: *The values shown by black ink and red ink inside brackets, represent the reduction percentage of the maximum structural responses compared with the uncontrolled case and the structure equipped with SATMD and non-simultaneous tuning related to [4], respectively.

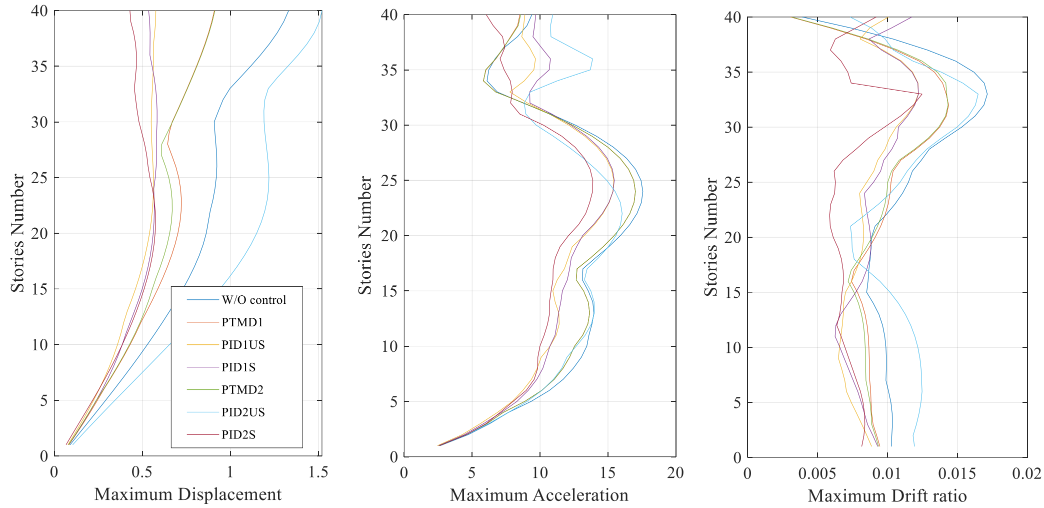

(a)

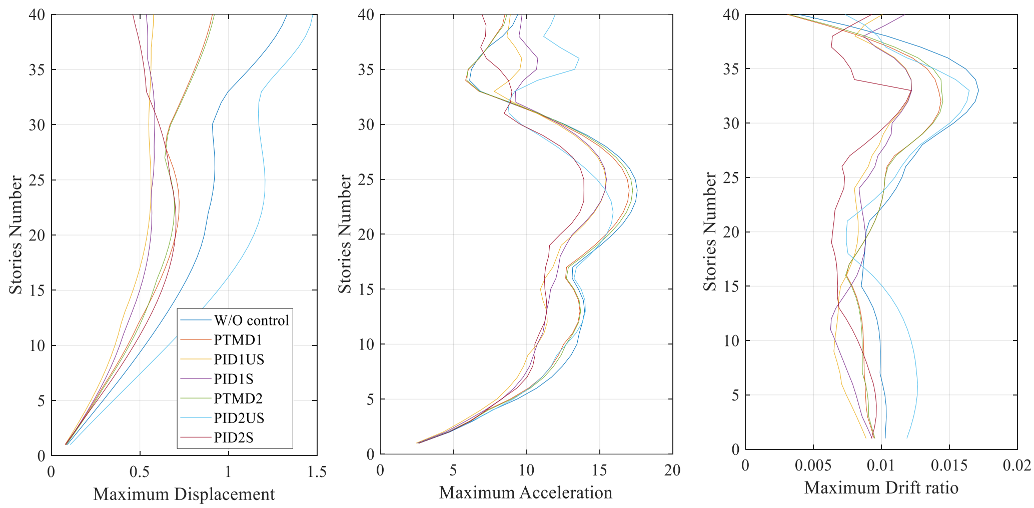

(b)

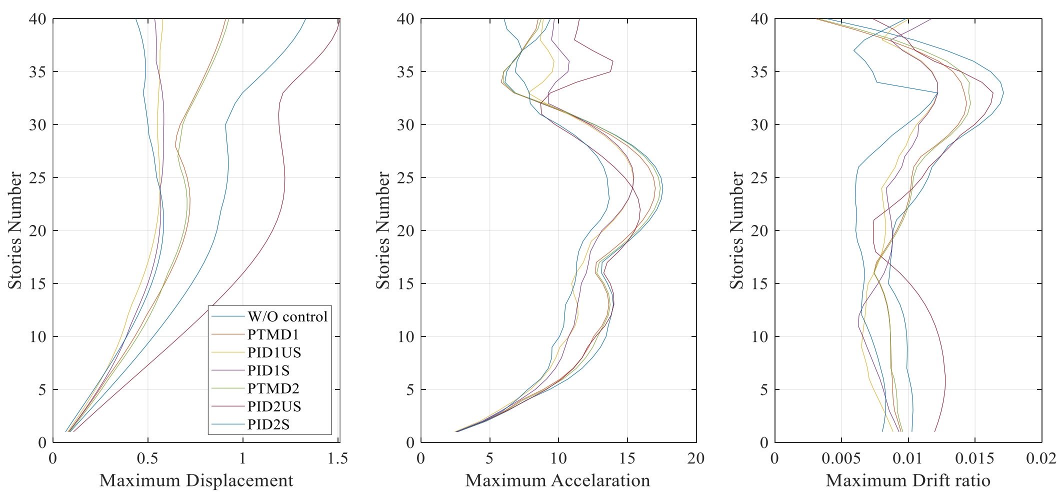

(c)

Fig. 6. Results of case 40-33 under the artificial earthquake: (a) Subcase 4-1, (b) Subcase 3-2, (c) Subcase 2.5-2.5

TABLE 9
RESULTS FOR ALL CASES UNDER THE KOBE EARTHQUAKE CONSIDERING SSI

Control case	Subcase	Non-simultaneous tuning			Simultaneous tuning		
		MAX. Disp(m)	MAX. Acc(m/s^2)	MAX. Drift ratio	MAX. Disp(m)	MAX. Acc(m/s^2)	MAX. Drift ratio
Uncontrolled	-	0.52	9.51	0.007	-	-	-
SPTMD [4]	-	0.47 (8.2%)	9.20 (3.3%)	0.0067 (6.9%)	-	-	-
SATMD (Non-simultaneous) [4]	-	0.33 (%)	8.97 (5.8%)	0.0063 (12.5%)	-	-	-
SATMD (Simultaneous	-	-	-	-	0.30 (41.0%,6.4%)*	8.93 (6.1%,3.3%)	0.0074 (-2.8%,17.5%)
MPTMD (case 40-33)	4-1	0.48 (7.8%)	9.20(3.3%)	0.0067 (6.9%)	-	-	-
	3-2	0.48 (7.2%)	9.25(2.8%)	0.0068 (5.6%)	-	-	-
	2.5-2.5	0.48 (6.9%)	9.29(2.3%)	0.0069 (4.2%)	-	-	-
MPTMD (case 40-25)	4-1	0.48 (7.6%)	9.21(3.2%)	0.0067 (6.9%)	-	-	-
	3-2	0.48 (7.0%)	9.26(2.7%)	0.0068 (5.6%)	-	-	-
	2.5-2.5	0.48 (6.6%)	9.29(2.3%)	0.0069 (4.2%)	-	-	-
MATMD (case 40-33)	4-1	0.42 19.0%, -28.6%)	**8.30 (12.7%, 7.4%)**	**0.0052 (27.8%, 17.5%)**	0.25 (51.5%, 23.0%)	8.55 (10.2%, 4.6%)	**0.006 (16.7%, 4.8%)**
	3-2	0.42 (18.8%, --29.0%)	**8.30 (12.7%, 7.4%)**	**0.0052 (27.8%, 17.5%)**	**0.24 (53.7%, 26.5%)**	8.63 (9.2%, 3.7%)	0.007 (16.7%, -3.2%)
	2.5-2.5	0.42 (18.6%, -29.3%)	**8.30 (12.8%, 7.4%)**	**0.0052 (27.8%, 17.5%)**	0.24 (52.9%, 25.2%)	**8.44 (11.3%, 5.9%)**	0.006 (15.3%, 3.2%)
MATMD (case 40-25)	4-1	0.57 (-9.4%, -73.8%)	10.15 (-6.7%, -11.7%)	0.0067 (6.9%, -6.0%)	0.29 (44.4%, 11.7%)	10.19 (-7.2%, -13.7%)	0.008 (-12.5%, -28.6%)
	3-2	0.57 (-9.3%, -73.6%)	10.18 (-7.0%, -13.5%)	0.0068 (5.6%, -7.9%)	0.33 (35.9%, -1.8%)	10.20 (-7.2%, -13.8%)	**0.006 (16.7%, 4.8%)**
	2.5-2.5	0.56 (-8.8%, -72.8%)	10.16 (-6.8, -13.3%)	0.0067 (6.9%, -6.3%)	0.34 (34.7%, -3.6%)	10.31 (-8.4%, -15.0%)	0.006 (15.3%, -3.2%)

However, the maximum drift ratio of the floors decreases by 15.3% and 16.7% for the mass ratio of 2.5%-2.5% and 3%-2% compared with the uncontrolled state.

Also, the best performance for the Newhall earthquake and all three essential responses is related to the structure equipped with MATMD and case 40-33 with simultaneous adjustment so that the maximum reduction was up to 66.7% for the maximum displacement, up to 14.1% for the maximum acceleration, and up to 26.5% for drift ratio compared with the uncontrolled state. It is noteworthy that this conclusion does not mean that case 40-25 did not improve the responses. For example, a reduction of up to 16.7% in the maximum displacement compared with SATMD with non-simultaneous tuning is observed for it. On the other hand, the responses were evaluated considering a trade-off between them. The selection criteria are based on the reduction of responses compared with the SATMD and non-simultaneous tuning. It shows that for the Kobe earthquake, maybe the best candidates for response improvement are related to MATMD with simultaneous tuning and case 40-33. The first selection may be the mass ratio of 2.5%-2.5% with a reduction of 25.2%, 5.9%, and 3.2% for three main maximum responses, respectively. The second choice is the mass ratio of 3%-2%, which entails a reduction of 26.5%, 3.7%, and 3.2% in the main maximum responses.

Similarly, for the Newhall earthquake, if considering a trade-off between responses, the best selection is the structure equipped with MATMD with simultaneous tuning related to case 40-33. As with the Kobe earthquake, the mass ratio of 2.5%-2.5% and 3%-2% are the best suggestions, and the highest reduction is generally 26.5%, 5.9%, and 4.8% for the main responses, respectively.

TABLE 10
RESULTS FOR ALL CASES UNDER THE NEWHALL EARTHQUAKE CONSIDERING SSI

Control case	Subcase	Non-simultaneous tuning			Simultaneous tuning		
		MAX. Disp	MAX. Acc	MAX. Drift ratio	MAX. Disp	MAX. Acc	MAX. Drift ratio
Uncontrolled	-	0.82	10.19	0.008	-	-	-
SPTMD [4]	-	0.76 (7.9%)	9.99 (2.0%)	0.008 (4.8%)	-	-	-
SATMD (Non-simultaneous) [4]	-	0.38 (53.4%)	8.86 (13.1%)	0.0062 (25.3%)	-	-	-
SATMD (Simultaneous)	-	-	-	-	0.33 (60.0%,14.4%)*	9.61 (5.7%, -8.5%)	0.007 (13.2%, -16.1%)
MPTMD (case 40-33)	4-1	0.76 (7.2%)	9.98(2.0%)	0.008 (6.0%)	-	-	-
	3-2	0.76 (7.9%)	10.02(1.6%)	0.008 (3.6%)	-	-	-
	2.5-2.5	0.75 (9.0%)	10.05(1.4%)	0.008 (2.4%)	-	-	-
MPTMD (case 40-25)	4-1	0.77 (6.1%)	10.00(1.9%)	0.008 (6.0%)	-	-	-
	3-2	0.77 (6.2%)	10.04(1.4%)	0.008 (4.8%)	-	-	-
	2.5-2.5	0.77 (6.3%)	10.06(1.2%)	0.008 (4.8%)	-	-	-
MATMD (case 40-33)	4-1	0.52 (37.1%, -35.0%)	9.51 (6.6%, -7.4%)	0.007 (9.6%, -21.0%)	0.30 (63.0%, 20.7%)	8.83 (13.4%, 0.3%)	**0.006 (26.5%, 1.6%)**
	3-2	0.52 (36.7%, -35.7%)	9.52 (6.6%, -7.4%)	0.007 (9.6%, -21.0%)	**0.27 (66.7%, 28.6%)**	8.93 (12.4%, -0.8%)	0.006 (22.9%, -3.2%)
	2.5-2.5	0.52 (36.3%, -36.5%)	9.52 (6.6%, -7.5%)	0.007 (9.6%, -21.0%)	0.29 (65.1%, 25.3%)	**8.75 (14.1%, 1.2%)**	0.006 (25.3%, 0.0%)
MATMD (case 40-25)	4-1	0.51 (38.7%, -23.9%)	9.87 (3.1%, -10.3%)	0.007 (19.3%, -7.5%)	0.33 (61.1%,16.7%)	9.24 (9.3%, -4.3%)	0.008 (6.0%, -25.8%)
	3-2	0.50 (39.4%, -30.0%)	9.87 (3.2%, -11.4%)	0.007 (19.3%, -8.1%)	0.33 (59.8%, 13.7%)	9.25 (9.2%, -4.4%)	0.007 (20.5%, -6.4%)
	2.5-2.5	0.50 (39.2%, -30.0%)	9.85 (3.3, -11.2%)	0.007 (19.3%, -8.1%)	0.33 (59.9%, 13.9%)	9.21 (9.6%, -4.02%)	0.007 (20.5%, -6.4%)

It is also important to evaluate the responses during the time history of an earthquake. One of the criteria to examine is the root mean square (RMS) presented in Eq. 16 for displacement responses. This equation can be generalized for acceleration and drift ratio responses.

$$x_{RMS} = \sqrt{\frac{{x_1}^2 + {x_2}^2 + \cdots + {x_n}^2}{n}} \qquad (16)$$

where x and n are the displacement response at time t and the number of input earthquakes, respectively. RMSs of the three main responses are shown in Figs. 8 and 9 for the Kobe and

Newhall earthquakes, respectively. The average RMS of the responses of floors is also presented as another indicator in Figs. 10 and 11.

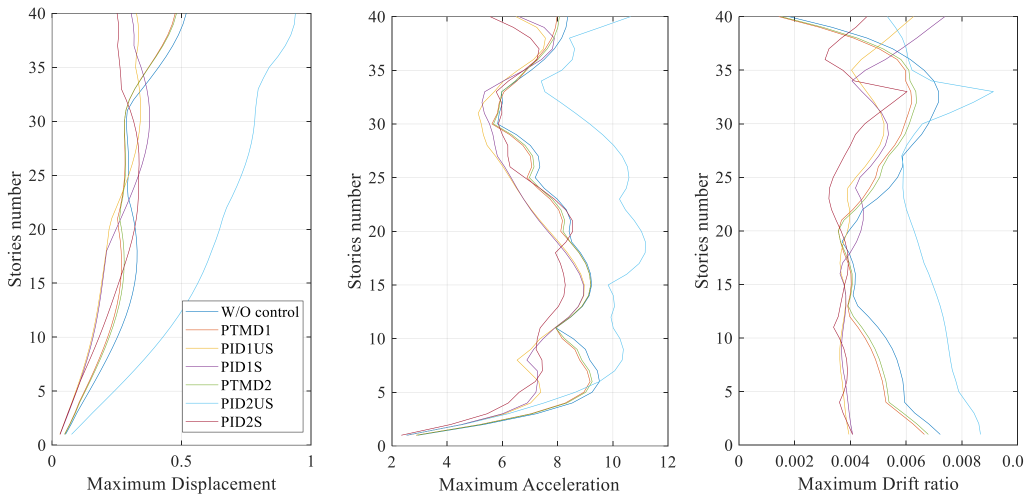

(a)

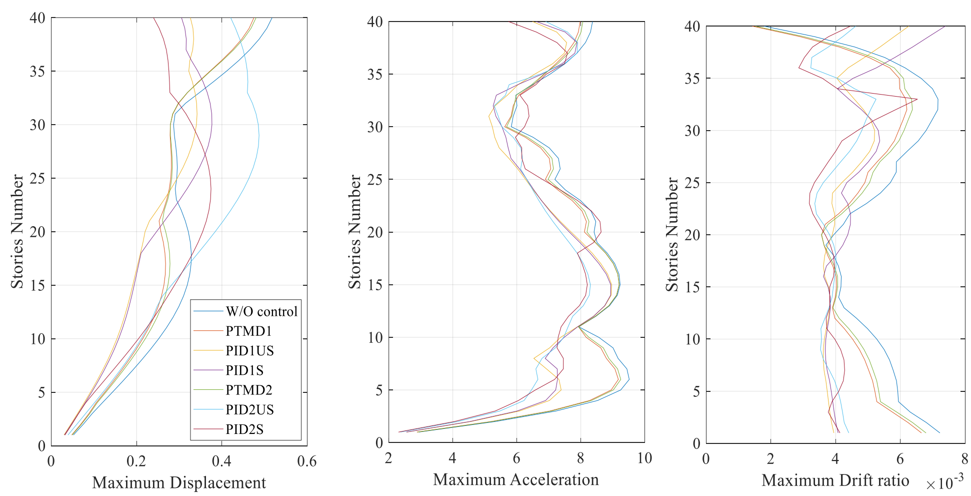

(b)

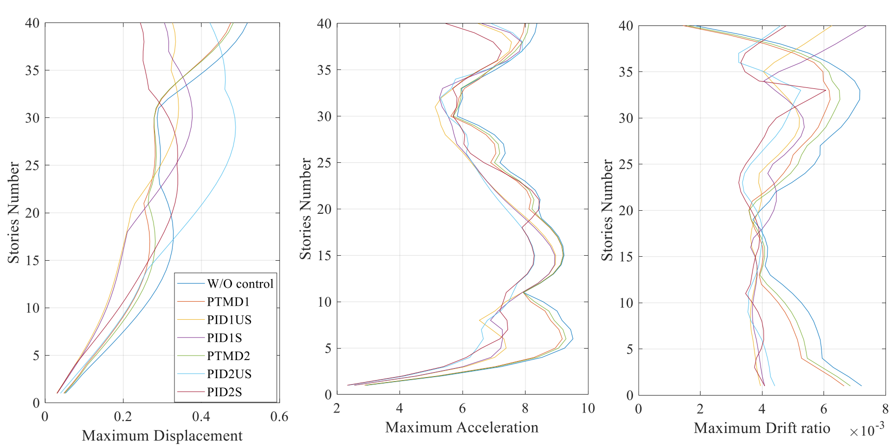

(c)

Fig. 7. Results for case 40-33 under the Kobe earthquake: (a) Subcase 4-1, (b) Subcase 3-2, (c) Subcase 2.5-2.5

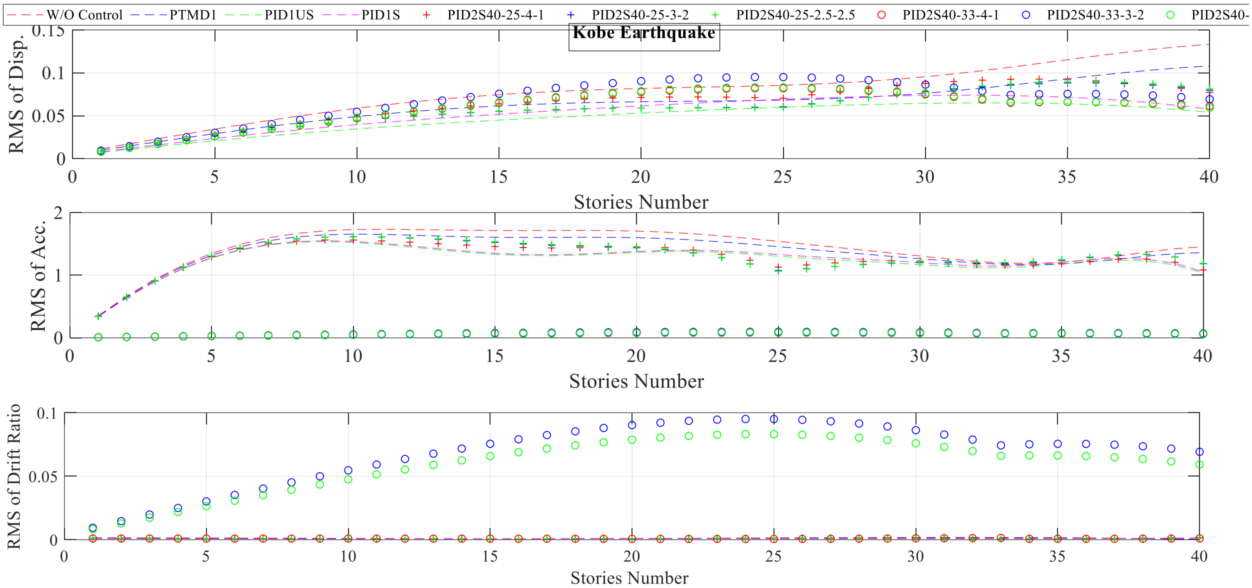

Fig. 8. Results of RMS for all stories under the Kobe earthquake

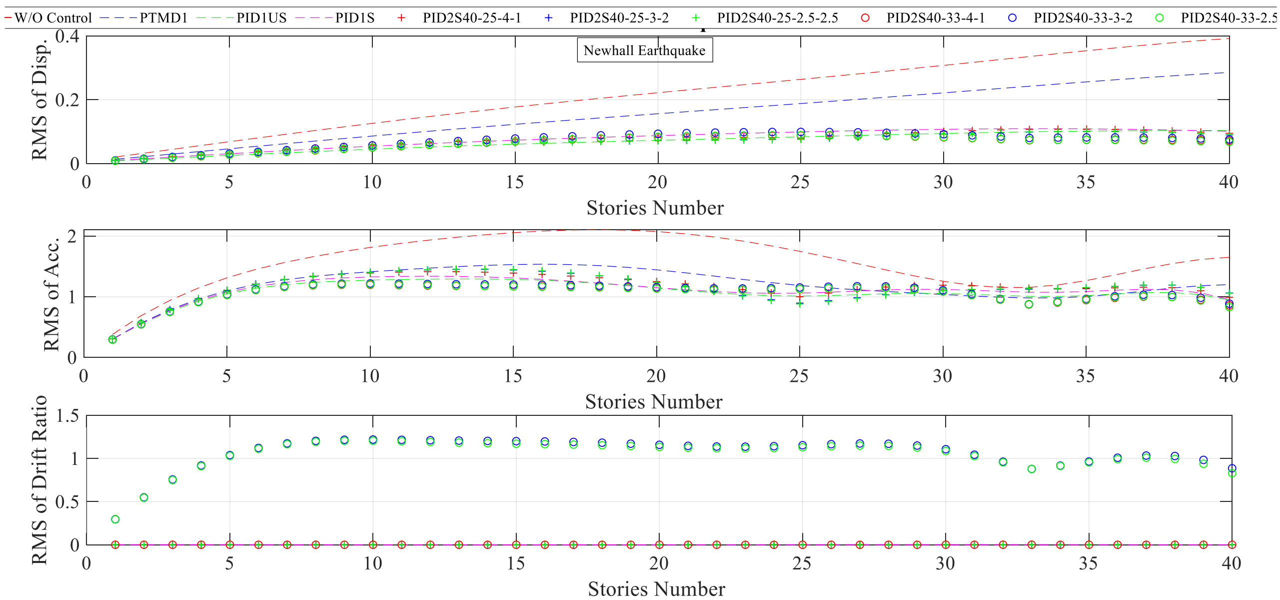

Fig. 9. Results of RMS for all stories under the Newhall earthquake

For the Newhall earthquake, the lowest maximum RMS of displacement and acceleration of the floors are related to MATMD and case 40-33 for which the values of 0.09 and 1.20 were gained, respectively. It belongs to the mass ratio of 4%-1%. In addition, the minimum RMS for the relative drift is 0.0014, related to SATMD with non-simultaneous tuning.

Also, for the Kobe earthquake, the best RMS for displacement and relative drift ratio are 0.065 and 0.0013, respectively. It belongs to SATMD with non-simultaneous tuning. In addition, for acceleration, case 40-33 and the mass ratio of 4%-1% are reported to have the best RMS of 1.514. Also, the lowest average RMS value of the response for the Kobe earthquake is related to SATMD with simultaneous tuning. Of course, the results of other active control states and different mass ratios are also very close to this value. On the contrary, the lowest average RMS is related to case 33-40, and the mass ratio 4%-1% for the Newhall earthquake and for three main responses.

VII. Conclusions

In this research, an innovative application-modification process was suggested. According to this, a new method was presented to find the TMDs' elevation placement position as a control device, could imrove responses and significantly reduces the volume of calculations, especially for the optimization process. In this regard, a few items were examined as follows: the effects of simultaneous and non-simultaneous designed parameters of PID and devices controller, various devices containing SPTMD, SATMD, MATMD, MPTMD, and different mass ratios. According to this proposed method, the mode shapes of the structure and the maximum responses in uncontrolled states were examined; In addition, the responses of the structure equipped with SPTMD and SATMD were considered taking SSI into account. Based on that, two placement scenarios were proposed. A 40-story tall benchmark structure located on soft soil was selected. For generalizing settings, a filtered white noise was applied as an artificial earthquake to the main structure, and design parameters were optimized using the PSO algorithm. to evaluate of the optimum settings, two famous Kobe-1995 and Northridge-1994 earthquakes were used and the results were presented.

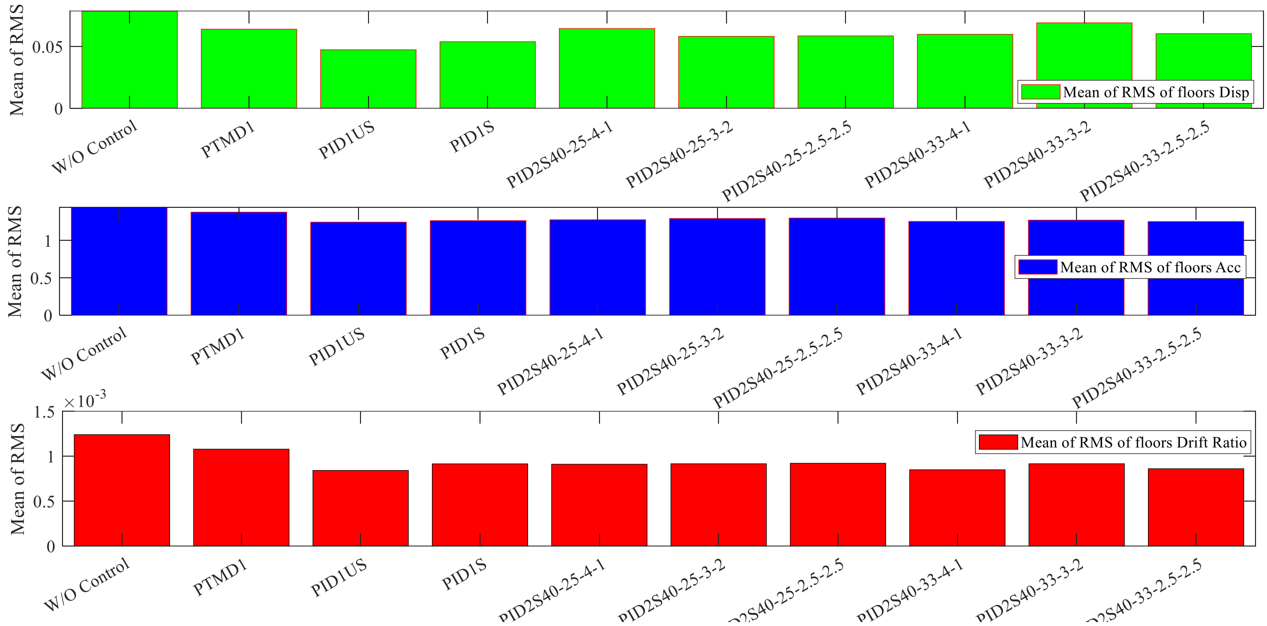

Fig. 10. Results of the mean of RMS of stories under the Kobe earthquake

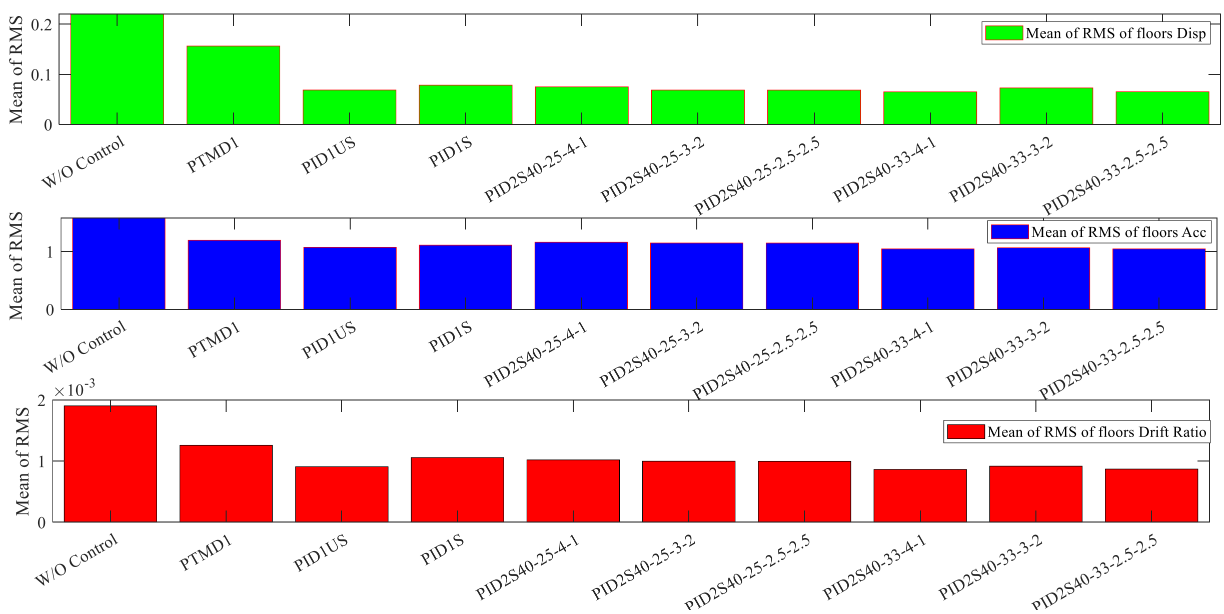

Fig. 11. Results of the mean of RMS of stories under the Newhall earthquake

The results of the application of the simultaneous tuning compared to non-simultaneous showed a significant decrease in the responses, especially, for the structure equipped with SATMD and MATMD taking SSI into account. It can increase the potential for structural instability. Also, two different scenarios were suggested to evaluate placement control devices. The results of using MPTMD instead of SPTMD were almost unchanged, provided that the total mass of TMDs was limited to 5% of the total mass of the structure. Further, the application of MATMD with PID controller and simultaneous tuning led to a significant improvement in the responses. These responses contained the maximum displacement, maximum acceleration, and maximum drift ratio. Also, to examine the effectiveness, the results were compared with the state of SATMD and PID controller with non-simultaneous tuning. In addition, the RMS of the floors and the average RMS of the total floors were investigated. Its criterion was used to evaluate the performance of the system in reducing the responses during the time history. The results confirmed the higher effectiveness of the controller and MATMD with the proposed elevation placement in improving responses; The general evaluation of the results showed that MATMD with simultaneous tuning in case 40-33 had the best application. Also, these results confirmed the superiority of MATMD and the proposed placements compared with SATMD [4]. Furthermore, the proposed method reduced requirement costs, especially for the optimization process. At last, the results will help designers and researchers to gain a new design vision to find the optimal placement of control devices in tall buildings.

Funding:

The authors received no financial support.

Declarations:

Conflict of interest the authors declare that have no conflict of interest or competing interests.

REFERENCES

[1] Liu, Ming-Yi., Chiang, W.-L., Hwang, J.-H., and Chu, C.-R., "Wind-Induced Vibration of High-Rise Building with Tuned Mass Damper Including Soil–Structure Interaction." Journal of Wind Engineering and Industrial Aerodynamics, vol. 96, no. 6-7, pp. 1092-102, 2008.

[2] Chey, Min-Ho and Jae-Ung Kim. "Parametric Control of Structural Responses Using an Optimal Passive Tuned Mass Damper under Stationary Gaussian White Noise Excitations." Frontiers of Structural and Civil Engineering, vol. 6, pp. 267-80, 2012.

[3] Nigdeli, Sinan Melih and Gebrail Bekdaş. "Optimum Tuned Mass Damper Design in Frequency Domain for Structures." KSCE journal of civil engineering, vol. 21, pp. 912-22, 2017.

[4] Shahi, Mohammad., Sohrabi, M. R., and Etedali, S., "Seismic Control of High-Rise Buildings Equipped with Atmd Including Soil-Structure Interaction Effects." Journal of Earthquake and Tsunami, vol. 12, no. 03, p. 1850010, 2018.

[5] Etedali, Sadegh and Mohammad Shahi. "A Control Scheme for Amd in the Presence of Time-Delays and Ssi Effects for Tall Buildings." Structural Engineering and Mechanics, An Int'l Journal, vol. 79, no. 2, pp. 267-78, 2021.

[6] Samali, Bijan., Al-Dawod, B. M., Kwok, K. C., and Naghdy, F. "Active Control of Cross Wind Response of 76-Story Tall Building Using a Fuzzy Controller." Journal of engineering mechanics, vol. 130, no. 4, pp. 492-98, 2004.

[7] Warsewa, Alexander., Wagner, J. L., Böhm, M., Sawodny, O., and Tarín, C. "Decentralized Lqg Control for Adaptive High-Rise Structures." IFAC-PapersOnLine, vol. 53, no. 2, pp. 9131-37, 2020.

[8] Mac, Thi-Thoa and Hai-Le Bui. "Lqr Control Design in Vibration Control of a Benchmark Building Structure Subjected to Seismic Load." The AUN/SEED-Net Joint Regional Conference in Transportation, Energy, and Mechanical Manufacturing Engineering: Proceeding of RCTEMME2021, Hanoi, Vietnam, Springer, pp. 771-80, 2022.

[9] Jalali, Himan Hojat., Farzam, M. F., Gavgani, S. A. M., and Bekdaş, G. "Semi-Active Control of Buildings Using Different Control Algorithms Considering Ssi." Journal of Building Engineering, vol. 67, p. 105956, 2023.

[10] Huo, Linsheng et al. "Robust Control Design of Active Structural Vibration Suppression Using an Active Mass Damper." Smart materials and structures, vol. 17, no. 1, p. 015021, 2007.

[11] Park, SJ et al. "Numerical and Experimental Investigation of Control Performance of Active Mass Damper System to High-Rise Building in Use." Wind & structures, vol. 12, no. 4, pp. 313-32, 2009.

[12] Li, Zhijun and Hojjat Adeli. "New Adaptive Robust H∞ Control of Smart Structures Using Synchrosqueezed Wavelet Transform and Recursive Least-Squares Algorithm." Engineering Applications of Artificial Intelligence, vol. 116, p. 105473, 2022.

[13] Shariatmadar, Hashem and H Meshkat Razavi. "Seismic Control Response of Structures Using an Atmd with Fuzzy Logic Controller and Pso Method." Struct. Eng. Mech, vol. 51, no. 4, pp. 547-64, 2014.

[14] Lavassani, S. H. H., Ebadijalal,M., Shahrouzi, M., Gharehbaghi, V., Farsangi, E. N., and Yang, T., "Interpretation of Simultaneously Optimized Fuzzy Controller and Active Tuned Mass Damper Parameters under Pulse-Type Ground Motions." Engineering Structures, vol. 261, p. 114286, 2022.

[15] Zamani, A. A., Tavakoli, S., and Etedali, S. "Control of Piezoelectric Friction Dampers in Smart Base-Isolated Structures Using Self-Tuning and Adaptive Fuzzy Proportional–Derivative Controllers." Journal of Intelligent Material Systems and Structures, vol. 28, no. 10, pp. 1287-302, 2017.

[16] Etedali, S., Tavakoli, S., and Sohrabi, M. R. "Design of a Decoupled Pid Controller Via Mocs for Seismic Control of Smart Structures." Earthquakes and Structures, vol. 10, no. 5, pp. 1067-87, 2016.

[17] Kayabekir, A. E., Bekdaş, G., Nigdeli, S. M. "Control of Reinforced Concrete Frame Structures Via Active Tuned Mass Dampers." Proceedings of 7th International Conference on Harmony Search, Soft Computing and Applications: ICHSA 2022, Springer, 2022, pp. 271-77.

[18] Etedali, Sadegh., Zamani, A.-A., and Tavakoli, S. "A Gbmo-Based Piλdμ Controller for Vibration Mitigation of Seismic-Excited Structures." Automation in Construction, vol. 87, pp. 1-12, 2018.

[19] Seghir, Jaballah Mohamed., Bachir, N., Salaheddine, H., and Salim, G. "Hybrid Vibration Control of Structures Using

Fractional Order Pi^\Uplambda D^\Upmu Pi Λ D M Controller." Artificial Intelligence and Heuristics for Smart Energy Efficiency in Smart Cities: Case Study: Tipasa, Algeria, Springer, pp. 569-77, 2022.
[20] Zamani, Abbas-Ali and Sadegh Etedali. "Optimal Fractional-Order Pid Control Design for Time-Delayed Multi-Input Multi-Output Seismic-Excited Structural System." Journal of Vibration and Control, vol. 29, no. 3-4, pp. 802-19, 2023.
[21] Akyürek, Osman. "Analysis of Different Placement Strategies of Multi-Tuned Mass Dampers Placed in Building Height." Arabian Journal for Science and Engineering, pp. 1-19, 2022.
[22] Etedali, Sadegh. "Probabilistic Study on Buildings with Mtmd System in Different Seismic Performance Levels." Structural Engineering and Mechanics, vol. 81, no. 4, pp. 429-41, 2022.
[23] Zhan, Wei., Cui, Y., Feng, Z., Cheung, K., Lam, J., and Gao, H. "Joint Optimization Approach to Building Vibration Control Via Multiple Active Tuned Mass Dampers." Mechatronics, vol. 23, no. 3, pp. 355-68, 2013.
[24] Huu, Thang Pham., Miura, N., and Iba, D. "Multi Active Tuned Mass Dampers for Earthquake-Induced Vibration Response Control of High Rise Building." Journal of Mechanical Science and Technology, vol. 36, no. 4, pp. 1655-66, 2022.
[25] Elias, Said., Matsagar, V., and Datta, T. "Distributed Tuned Mass Dampers for Multi-Mode Control of Benchmark Building under Seismic Excitations." Journal of Earthquake Engineering, vol. 23, no. 7, pp. 1137-72, 2019.
[26] Golnargesi, Siamak et al. "Seismic Control of Buildings with Active Tuned Mass Damper through Interval Type-2 Fuzzy Logic Controller Including Soil–Structure Interaction." Asian Journal of Civil Engineering, vol. 19, no. 2, pp. 177-88, 2018.
[27] Mishra, Abhishek., Shukla, A., Shukla, M., and Vanshaj, K. "Salp Swarm Optimization of Active Tuned Mass Dampers in Asymmetric Plan Buildings Including Ssi Effects." Asian Journal of Civil Engineering, vol. 24, no. 3, pp. 837-48, 2023.
[28] Etedali, Sadegh., Sohrabi, M. R., and Tavakoli, S. "Optimal Pd/Pid Control of Smart Base Isolated Buildings Equipped with Piezoelectric Friction Dampers." Earthquake Engineering and Engineering Vibration, vol. 12, pp. 39-54, 2013.
[29] Ulusoy, Serdar., Nigdeli, S. M., and Bekdaş, G. "Novel Metaheuristic-Based Tuning of Pid Controllers for Seismic Structures and Verification of Robustness." Journal of Building Engineering, vol. 33, p. 101647, 2021.
[30] Kennedy, James and Russell Eberhart. "Particle Swarm Optimization." Proceedings of ICNN'95-international conference on neural networks, vol. 4, IEEE, pp. 1942-48, 1995.
[31] Fourie, PC and Albert A Groenwold. "The Particle Swarm Optimization Algorithm in Size and Shape Optimization." Structural and Multidisciplinary Optimization, vol. 23, no. 4, pp. 259-67, 2002.
[32] Schutte, Jaco F and Albert A Groenwold. "Sizing Design of Truss Structures Using Particle Swarms." Structural and Multidisciplinary Optimization, vol. 25, pp. 261-69, 2003.
[33] Leung, Andrew Yee Tak and Haijun Zhang. "Particle Swarm Optimization of Tuned Mass Dampers." Engineering Structures, vol. 31, no. 3, pp. 715-28, 2009.
[34] Mohan, SC et al. "A Comparative Study on Crack Identification of Structures from the Changes in Natural Frequencies Using Ga and Pso." Engineering Computations, 2014.
[35] Khatir, Samir et al. "Multiple Damage Detection in Composite Beams Using Particle Swarm Optimization and Genetic Algorithm." Mechanics, vol. 23, no. 4, pp. 514-21, 2017.
[36] Ghannadi, Parsa et al. "The Application of Pso in Structural Damage Detection: An Analysis of the Previously Released Publications (2005–2020)." Frattura ed Integrità Strutturale, vol. 16, no. 62, pp. 460-89, 2022.
[37] Saidi, Hanane et al. "Energy Spectra of the Schrödinger Equation and the Differential Quadrature Method: Improvement of the Solution Using Particle Swarm Optimization." Applied mathematics and computation, vol. 182, no. 1, pp. 559-66, 2006.
[38] De Falco, Ivanoe et al. "Facing Classification Problems with Particle Swarm Optimization." Applied Soft Computing, vol. 7, no. 3, pp. 652-58, 2007.
[39] He, Qie and Ling Wang. "An Effective Co-Evolutionary Particle Swarm Optimization for Constrained Engineering Design Problems." Engineering Applications of Artificial Intelligence, vol. 20, no. 1, pp. 89-99, 2007.
[40] Leung, Andrew Yee Tak and Haijun Zhang. "Particle Swarm Optimization of Tuned Mass Dampers." Engineering Structures, vol. 31, no. 3, pp. 715-28, 2009.
[41] Shi, Yuhui and Russell Eberhart. "A Modified Particle Swarm Optimizer." 1998 IEEE international conference on evolutionary computation proceedings. IEEE world congress on computational intelligence (Cat. No. 98TH8360), IEEE, pp. 69-73, 1998.
[42] Eberhart, Russell C and Yuhui Shi. "Tracking and Optimizing Dynamic Systems with Particle Swarms." Proceedings of the 2001 congress on evolutionary computation (IEEE Cat. No. 01TH8546), vol. 1, IEEE, pp. 94-100, 2001.
[43] Mirzaei, Davoud and Saeid Amini. "Design a Novel Ultrasonic Horn Using Electro-Mechanical Circuit Method and Optimization Algorithm." International Journal of Industrial Electronics Control and Optimization, vol. 5, no. 3, pp. 269-77, 2022.
[44] Hosseini Lavassani, Seyed Hossein and Saman Shangapour. "Interval Type-2 Fuzzy Hybrid Control of a High-Rise Building Including Soil–Structure Interaction under near-Field and Far-Field Ground Motions." Structural Engineering International, vol. 32, no. 3, pp. 316-27, 2022.
[45] Arfiadi, Y., & Hadi, M. "Optimum placement and properties of tuned mass dampers using hybrid genetic algorithms." Iran University of Science & Technology, 1(1), 167-187, 2011.
[46] Alberto, P., Sala, A., & Olivares, M. " Fuzzy Logic Controllers. Methodology. Advantages and Drawbacks". In, 2015.
[47] Radmard Rahmani, H., & Könke, C. "Seismic control of tall buildings using distributed multiple tuned mass dampers." Advances in Civil Engineering, pp. 1-19, 2019.
[48] Azizi, M., Talatahari, S., & Sareh, P. (2022). Design optimization of fuzzy controllers in building structures using the crystal structure algorithm (CryStAl). Advanced Engineering Informatics, 52, 101616.

Mohammad Shahi was born in Iran in 1985. He received his B.Sc. degree in Civil Engineering from the Torbat Heydarieh University, Torbat Heydarieh in 2010 and his M.Sc. degree in Structural Engineering from University of Sistan and Baluchestan, Zahedan, Iran in 2017. He is a Ph.D. candidate in Structural Engineering at University of Sistan and Baluchestan , Zahedan. His current research interests include the structural control in smart structures.

Mohammad Reza Sohrabi received B.Sc., M.Sc. degrees in Civil Engineering from the University of Tehran, Tehran, Iran in 1984 and 1986 respectively. His current research interests include the structural control in smart structures. He received Ph.D. degree in structural engineering from University of Newcastle Upon Tyne in 1996. Currently, he is an associated professor at the Engineering Faculty of University of Sistan and Baluchestan, Zahedan, Iran. His research interests include structural contro l, Concrete structure s and structural dynamics.

Sadegh Etedali was born in Zahedan, Iran on January 2, 1983. Sadegh Received his Ph.D. degree in Structural Engineering from the University of Sistan and Baluchestan, Zahedan, Iran in 2014. After graduation, Sadegh Joined the Department of Civil Engineering at the Birjand University of Technology (BUT), Birjabd, Iran. He is currently an associate professor in the Department of Civil Engineering, BUT. Dr. Etedali has more than 8 years of experience in the field of structural vibration and control, soil - structure interaction, smart structures, soft computing, structural optimization, and structural reliability. He has published more than 80 scientific papers in journals and proceedings at national and international levels. He supervised/advised 15 M.Sc. and 5 Ph.D. students.

Abbas -Ali Zamani was born in Isfahan, Iran, in 1986. He received the B.Sc. degree in Electronic Engineering from Hakim Sabzevari University, Sabzevar, Iran 2009. He received the M.Sc. degree from Isfahan University of Technology, Isfahan, Iran 2011, and the Ph.D. degree from the University of Sistan and Baluchestan, Sistan and Baluchestan, Iran, in 2018, in Control Engineering. He is an Assistant Professor in the Department of Electrical Engineering, Technical and Vocational University, Isfahan, Iran. His research interests are Seismic Control, Power System Control, Smart grids, Renewable energies, and Artificial intelligence.